

Preparation and synthesis of the nanoferrite $\text{Ni}_{0.3}\text{Co}_{0.2}\text{Zn}_{0.5}\text{Al}_x\text{Fe}_{2-x}\text{O}_4$ utilizing sol-gel auto-combustion approach

R. A. Munef^{*}, B. A. Omar, S. J. Fathi

Dept. of Physics, College of Science, University of Kirkuk, Kirkuk, Iraq

Nanoferrite, which has the chemical structure ($\text{Ni}_{0.3}\text{Co}_{0.2}\text{Zn}_{0.5}\text{Al}_x\text{Fe}_{2-x}\text{O}_4$), have been produced with the use of the sol-gel auto-combustion approach that have ($X=0, 0.1, 0.2, 0.3, 0.4$ and 0.5) values. Samples are calcined at a temperature of ($1,250^\circ\text{C}$) for a duration of (2 h), structure characteristics of the ferrite was confirmed by XRD. The results of the XRD have shown that the ferrite that has a size of the grain that ranges between (22 nm and 40 nm) and have a spinel Cubic phase, the x-ray result density ($\rho_{x\text{-ray}}$) has been decreased with the content of Al^{+3} . Electrical properties have shown that the dielectric loss factor and dielectric constant are reduced with an increase in frequency. Conductivity increases as well ($\sigma_{a.c}$) with the increase in the frequency value.

(Received December 22, 2021; Accepted April 1, 2022)

Keywords: Ferrites, Al^{+3} ions, Sol -gel method, SEM, Electrical properties, XRD

1. Introduction

Ferrites are a set of the semiconductor oxides, and it's of a high significance, due to the fact that it is highly resistive and has good magnetic characteristics [1]. NiFe_2O_4 ferrites have a spinel structure and they are materials which are highly resistant up to (10^9 m Ω) [2]. The chemical composition, micro-structure and synthesis method are significant for the ferrites' electrical properties [3]. For the purpose of obtaining the optimal magnetic and electrical characteristics have to be interchange coupling between the soft and the hard ferrites [4-7]. Several of methods such as the solid state reactions, Hydrothermal, sol-gel and also sol-gel Auto Combustion approach were utilized for the purpose of synthesizing soft spinel ferrite materials [8-10]

2. Experimental methods

2.1. Materials and synthesis

Nanoferrites of compound ($\text{Ni}_{0.3}\text{Co}_{0.2}\text{Zn}_{0.5}\text{Al}_x\text{Fe}_{2-x}\text{O}_4$) ($X=0, 0.1, 0.2, 0.3, 0.4$ and 0.5) have been produced with the use of the approach of the sol-gel auto-combustion by the following raw materials that will be mentioned. The analytical grade nickel nitrate [$\text{Ni}(\text{NO}_3)_2 \cdot 6 \text{H}_2\text{O}$], copper nitrate [$\text{Co}(\text{NO}_3)_2 \cdot 3 \text{H}_2\text{O}$], zinc nitrate [$\text{Zn}(\text{NO}_3)_2 \cdot 6 \text{H}_2\text{O}$], citric acid [$\text{C}_6\text{H}_8\text{O}_7$], iron nitrate [$\text{Fe}(\text{NO}_3)_3 \cdot 9 \text{H}_2\text{O}$], and Aluminum nitrate [$\text{Al}(\text{NO}_3)_3 \cdot 9 \text{H}_2\text{O}$] have been utilized for the preparation of the ($\text{Ni}_{0.3}\text{Co}_{0.2}\text{Zn}_{0.5}\text{Al}_x\text{Fe}_{2-x}\text{O}_4$) ferrite with $x = 0, 0.10, 0.20, 0.30, 0.40$ and 0.50 compositions. The metal nitrates and the citric acid have been dissolved in the de-ionized water, all those have been gathered in a glass beaker and thoroughly mixed at the temperature of the room through the use of the magnetic stirrers, a solution for Ammonia has been gradually added to the mixed solution the purpose of controlling its value of pH to the point of reaching the value of (7) with the continuous rotations. The temperature has been increased gradually until reaching 80°C for the purpose of to transform it to gel and after that, ignited in self propagating combustion way for the purpose of forming a loose fluffy powder. As-burnt precursor powder has been calcined after that, at a temperature of $1,250^\circ\text{C}$ for a 2h duration. The powder has been pressed with the use

^{*} Corresponding authors: rafeamonef@uokirkuk.edu.iq
<https://doi.org/10.15251/JOR.2022.182.213>

of a die that has a (1.50 cm) diameter for the purpose of to pellet-shaped specimens. The utilized load of the pressing has been (7 ton) and specimens have been held under pressure for 1 min with the use of a hydraulic press of a 15 ton maximal load.

2.2. Characterization

The prepared nano ferrites' structural characterization has been carried out through the use of the XRD analysis that confirmed the formation of the phase. The prepared nano ferrites' dielectric characteristics have assessed with the use of the LCR meter that ranged between 50 KHz and 1 MHz. The dielectric parameters like the dielectric loss tangent ($\tan \delta$) and dielectric constant (ϵ'), have evaluated with the use of the LCR meter.

3. Results and discussion

The $\text{Ni}_{0.3}\text{Co}_{0.2}\text{Zn}_{0.5}\text{Al}_x\text{Fe}_{2-x}\text{O}_4$ Nanoferrites' XRD patterns, for samples with $x = 0, 0.10, 0.20, 0.30, 0.40$ and 0.50 Fig2 shows that the patterns of the XRD have one Cubic phase and the peaks' intensity has been increased with the increase of the concentration of the Al ion. After that, the observed peaks of diffraction may be assigned to (111), (022), (113), (222), (004), (224), (333), (044) and (533) reflection plane. Comparing the XRD results to the (JCPD052-0278) has shown that 3 peaks (421), (201), and (310) and returned to (Fe_2O_3).

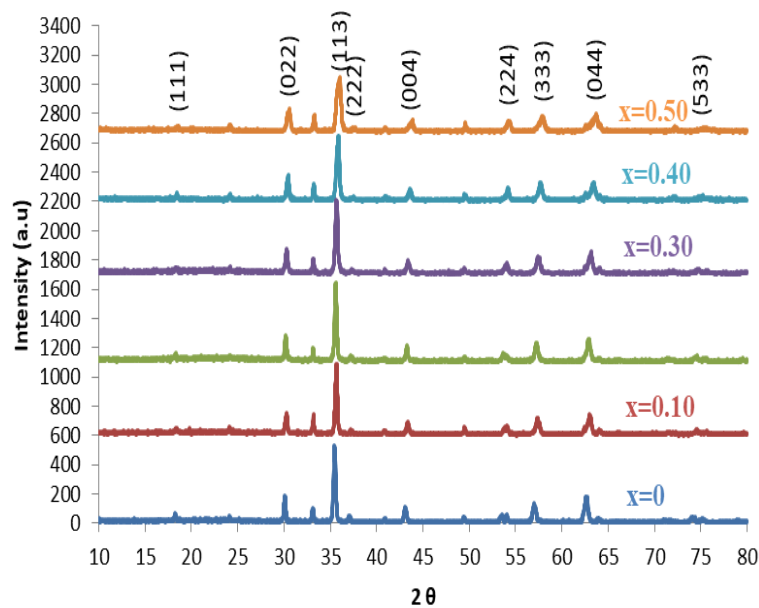


Fig. 1. Patterns of XRD for $\text{Ni}_{0.3}\text{Co}_{0.2}\text{Zn}_{0.5}\text{Al}_x\text{Fe}_{2-x}\text{O}_4$ sample

The individual composition lattice parameter has been researched with the use of the equation below: [13].

$$d_{hkl} = \frac{a}{\sqrt{h^2 + k^2 + l^2}} \quad (1)$$

d: represents inter- planar distance.

a: represents lattice constant.

(h, k, l): represent Miller indices

Scherer's equation has been used for the determination of the sample's average size of the crystallite [14].

$$D = K \lambda / \beta \cos(\theta) \quad (2)$$

D: represents crystallite size.

λ : represents wave-length of the x -ray (Cu α radiation, 01.5405Å^o).

θ : represents Bragg's angle.

β : represents full diffraction line width at half of maximal intensity that has been measured with the radians.

Williamson-Hall equation

$$B \cos\theta = k\lambda/D_{w-H} + 4 \varepsilon \sin(\theta) \quad (3)$$

The samples' actual density of the (X-ray) has been specified with the use of the equation [15],

$$\rho_{x-ray} = \frac{ZM_{wt}}{N_a V} \quad (4)$$

M: represents sample's molecular weight (Kg).

a : represents lattice parameter (Å).

N_a : represents Avogadro's number (per mol).

The noticed reduction in lattice constant (a) that could be related to an increase in the Al⁺³ content the samples' crystallite size has been noticed to be decreased with the concentration of Al. The density of the X-ray is linearly decreased with the concentration of Al as can be seen in figure2.

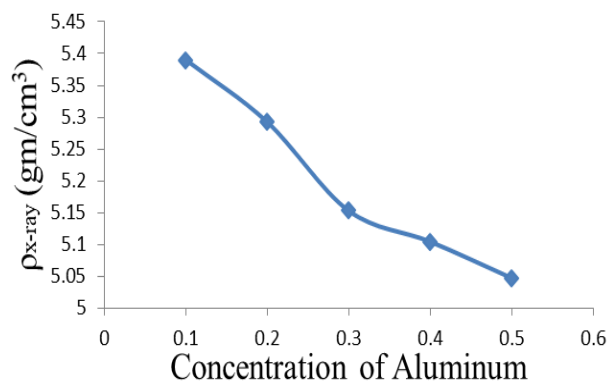


Fig. 2. Decrease of the density of the x-ray with increase in the concentration of Al⁺³.

Table 1. Al⁺³ doping effects upon crystalline size lattice parameter, and X-ray density of Ni_{0.3}Co_{0.2}Zn_{0.5}Al_xFe_{2-x}O₄ system.

Content of Al (x)	Lattice constant a (Å ^o)	c/a	C (Å ^o)	ρ_{x-ray} (g/cm ³)	Lattice volume V (Å ^{o3})
X = 0.00	8.38590	1.000	8.38590	5.37690	589.73420
X = 0.10	8.34510	1.000	8.34510	5.39010	581.17720
X = 0.20	8.36180	1.000	8.36180	5.29240	584.65880
X = 0.30	8.40150	1.000	8.40150	5.15290	593.03420
X = 0.40	8.39270	1.000	8.39270	5.10440	591.16000
X = 0.50	8.39180	1.000	8.39180	5.04730	590.98820

3.1. Scanning Electron Microscope (SEM)

By using the Scanning electron microscope we can locate the average crystallite size and morphology of the surface the details which we obtain by this technique are the grains distribution in addition to pores inside the granules, Fig (6) shows up SEM of the nano compound sample.

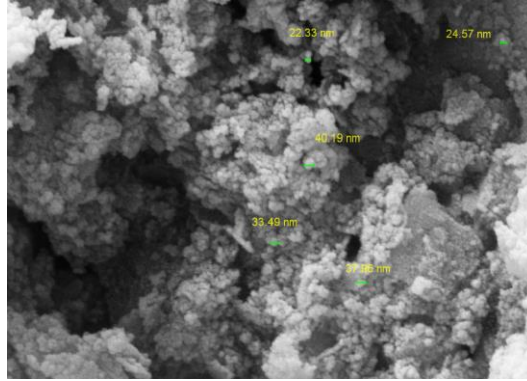


Fig. 6. SEM of $Ni_{0.3}Co_{0.2}Zn_{0.5}Al_{0.5}Fe_{1.5}O_4$ sample.

3.2. Electrical characteristics

Electrical characteristics of the Al doped NiCoZn ferrite ($Ni_{0.3}Co_{0.2}Zn_{0.5}Al_xFe_{2-x}O_4$), with ($X=0, 0.10, 0.20, 0.30, 0.40$ and 0.50) of the additions of the Al include dielectric characteristics, A.c conductivity.

3.3. Dielectric characteristics

The real dielectric constant's part ϵ' has been computed with the use of the following equation [16],

$$\epsilon'_r = \frac{ct}{\epsilon_0 A} \quad (5)$$

C: represents capacitance

d: represents thickness (cm)

A: represents surface area (cm^2)

ϵ_0 : represents the air dielectric permittivity ($8.8540 \times 10^{-14} F/cm$).

The dielectric loss's imaginary part ϵ'' has been computed with the use of the following equation [16]

$$\epsilon''_r = \tan \delta \epsilon'_r \quad (6)$$

Fig3 and Fig4 illustrate the dielectric constant's real and imaginary parts $\epsilon'_r, \epsilon''_r$ (the dependence of ($Ni_{0.3}Co_{0.2}Zn_{0.5}Al_xFe_{2-x}O_4$) on frequency ω , for a variety of the Al doping content. The dielectric constant's real and imaginary parts for all of the samples are reduced with the increase in the frequency. Such behavior has been in agreement with the relaxation process of Deby's type. The dielectric constant's real and imaginary parts reach a certain value for every sample that is higher than a specific higher frequency value, which has been in agreement with [17]. It may be seen in Figure4 that the dielectric constant's imaginary parts ϵ''_r , are increased with increase of the value of the frequency:

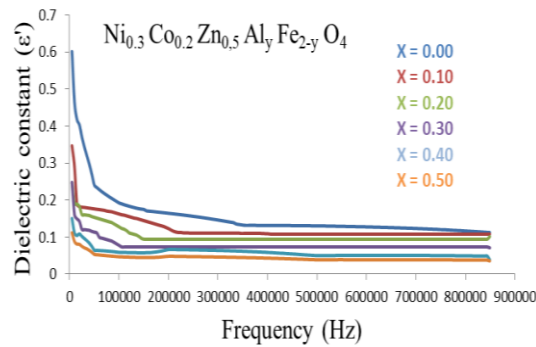


Fig. 3. Variations of the dielectric constant's real part (ϵ'_r) with the frequency for ($Ni_{0.3}Co_{0.2}Zn_{0.5}Al_xFe_{2-x}O_4$) at different x value.

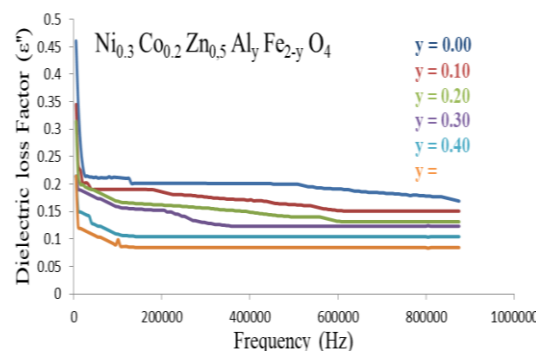


Fig. 4. Variations of the dielectric constant's imaginary part (ϵ''_r) with the frequency for ($Ni_{0.3}Co_{0.2}Zn_{0.5}Al_xFe_{2-x}O_4$) at a variety of the Aluminum contents.

3.4. A.C. Conductivity

AC conductivity has been evaluated with the use of the following equation [16],

$$\sigma_{a.c} = 2\pi f \epsilon_0 \epsilon'_r \tan \delta \quad (6)$$

Fig. 5 illustrates A.C. conductivity variations with frequency values (between 50 Hz and 1 MHz). A.C. conductivity increases with the increase in the frequency for all of the specimens, and that has been defined as the ferrites' normal behavior, which has agreed with [18].

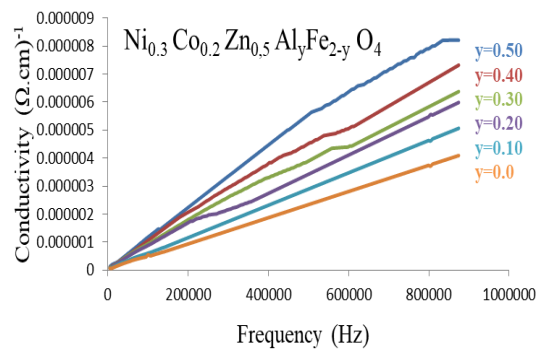


Fig. 5. AC conductivity as a frequency function for with ($Ni_{0.3}Co_{0.2}Zn_{0.5}Al_xFe_{2-x}O_4$) various Al contents.

4. Conclusion

In the present paper, $\text{Ni}_{0.3}\text{Co}_{0.2}\text{Zn}_{0.5}\text{Al}_x\text{Fe}_{2-x}\text{O}_4$ nano compound has been synthesized and synthesized with success with a different Al(x=0.10- 0.50) value with the use of the sol- gel autocombustion approach, From the pattern of the XRD the observed phase is Cubic, the Average crystallite is (22nm- 40 nm) with the use of the Williamson's Holl and Debay- sherer relations. The Dielectric loss and the Dielectric constant for each Sample have been decreased with the increase in the frequency and ratio of the overlay for reaching the minimal value at (Al =0.50) and a (1 MHz) frequency, and A.C. conductivity increases with an increase in the frequency and concentration of Aluminum for the purpose of reaching the maximal value at a (1 MHz) frequency and (Al =0.50).

References

- [1] R. C. Kambale, P. A. Shaikh, S. S. Kambale, Y. D. Kolekar, Journal of Alloys Compound, vol.478, pp.599-603,(2009); <https://doi.org/10.1016/j.jallcom.2008.11.101>
- [2] V. F. Belov, T. A. Khimich, M. N. Shipko, L. M. Letyuk, L. N. Korablin, E. V Korneev, Moscow Institute of Steel and Alloys, no.3, pp.77-81,(1973); <https://doi.org/10.1007/BF00895425>
- [3] A. Verma, R. Chatterjee, J. Magn. Mater. Vol. 306, PP. 313-320, (2006); <https://doi.org/10.1016/j.jmmm.2006.03.033>
- [4] Fenlian Zan, Yongqing Ma, Qian Ma, Yuanfeng Xu, Zhenxiang Dai, Ganhong Zheng, Mingzai Wu, Guang Li, J. Am. Ceram. Soc. ,pp:1-8(2013).
- [5] Bilal Ahmed Omar, Rabab Shakour Ali, NeuroQuantology, March 2021, Volume 19, Issue 3, Page 56-61, (2021); <https://doi.org/10.14704/nq.2021.19.3.NQ21028>
- [6] C. Morrison, L. Saharan, Y. Ikeda, K. Takano, G. Hrkac, T. Thomson, J. Phys. D. Appl. Phys., 46(47),pp:1-5,(2013); <https://doi.org/10.1088/0022-3727/46/47/475002>
- [7] J. Liu, H. Sepehri-Amin, T. Ohkubo, K. Hioki, A. Hattori, T. Schrefl, K. Hono, Acta Mater., 61(14), pp:5387-5399,(2013); <https://doi.org/10.1016/j.actamat.2013.05.027>
- [8] S. Pauline, Archives of Applied Science Research, 3 (5), pp:213-223, (2011).
- [9] A. Sutka, Iop Science Journal, (25), pp:1-12, (2011); <https://doi.org/10.1088/1757-899X/25/1/012019>
- [10] R. Elilarassi, G. Chandrasekaran, J. Mater. Sci. Mater. Electron., vol. 21, no. 11, pp. 1168-1173, (2010); <https://doi.org/10.1007/s10854-009-0041-y>
- [13] Collity BD. Elements of X-ray Diffraction. California: Addison – Wesley; (1978).
- [14] Bilal A.Omar, Sabah J.Fathi, Farouq I.Hussain, International Journal of Recent Research and Applied Studies, Volume 4, Issue 6 (17), June (2017) .
- [15] V. D. D Suryawanshi, R. Rajendra, B. Pushpinder, N. Rajlakshmi, Int. J. Chem. Phys. Sci. Spec. Issue – NCRTSM, vol. 3, pp. 2319–6602, 2014.
- [16] Bilal A.Omar, Sabah J. Fathi, Kareem A. Jassim, Technologies and Materials for Renewable Energy, Environment and Sustainability, vol.1968pp: 030047-1-030047-9,(2018); <https://doi.org/10.1063/1.5039234>
- [17] Kambale R C, Adhate N R, Chougule B K, Kolekar Y D J. Alloys Compd. 491 372,(2010); <https://doi.org/10.1016/j.jallcom.2009.10.187>
- [18] R. S. Devan, Y .D. Kolekar, B. K. Coagula, J. Physics: Condensed Matter, pp:18-43,(2006) <https://doi.org/10.1088/0953-8984/18/43/004>